www.sciencemag.org/content/348/6239/1115/suppl/DC1

Supplementary Materials for

Tuning friction atom-by-atom in an ion-crystal simulator

Alexei Bylinskii, Dorian Gangloff, Vladan Vuletić*

*Corresponding author. E-mail: vuletic@mit.edu

Published 5 June 2015, *Science* **348**, 1115 (2015)
DOI: 10.1126/science.1261422

This PDF file includes:

Materials and Methods
Fig. S1
References

Other Supplementary Material for this manuscript includes the following:
(available at www.sciencemag.org/cgi/content/full/348/6239/1115/DC1)

Database S1 as a zipped archive

Materials and Methods

Trapping Potentials

The one-dimensional corrugated potential V is produced by an intra-cavity optical standing wave superimposed on a linear Paul trap as described in detail in ref. (*23*). The TEM_{00} mode of the cavity is pumped by laser light blue-detuned by 12.7 GHz from the 369.5 nm $^2S_{1/2} \rightarrow {}^2P_{1/2}$ transition in $^{174}Yb^+$, resulting in optical-lattice potential minima at the nodes of the optical field. The corrugation parameter $\eta = (\omega_L / \omega_0)^2$ is defined in terms of the quantity $\omega_L = \sqrt{2\pi^2 U / (ma^2)}$, which is the oscillation frequency of an ion around an optical-lattice potential minimum in the harmonic approximation. The optical lattice coincides with the purely electrostatic axis of the Paul trap, along which the ions self-organize into a one-dimensional Coulomb crystal due to a much stronger transverse confinement by radio-frequency fields, with vibrational frequencies $\omega_{trans} / (2\pi)$ in excess of 1 MHz. Although the ions in a crystal interact via a long-range Coulomb force scaling as $\left|x_i - x_j\right|^{-2}$, it can be linearized for small ion displacements from equilibrium on the scale of the optical lattice spacing, resulting to leading order in spring forces between all ion pairs that fall off as the square of the inter-ion distance. While the Frenkel-Kontorova model assumes only nearest-neighbor spring forces, previous theoretical work (*19*) suggests that the FK model can effectively describe the long-range Coulomb system.

Raman Sideband Cooling

We cool the ions using a degenerate lattice-assisted Raman sideband cooling scheme *(23,31)* using the spin-1/2 Zeeman magnetic sublevels in $^{174}Yb^+$. The optical lattice described above, blue-detuned by 12.7 GHz, is slightly elliptically polarized. In a transverse magnetic field, the strong linearly polarized component and the weak circularly polarized component drive stimulated two-photon Raman transitions from $|n\rangle$ to $|n-1\rangle$ and $|n-2\rangle$ vibrational levels and flip the electronic spin. A circularly polarized laser beam collinear with the magnetic field and red-detuned by 100 MHz repumps the ion to the initial magnetic sublevel via a spontaneous two-photon Raman process, resulting in fluorescence which we collect. This fluorescence is modulated by a sinusoidally-varying (in space) coupling of the off-resonant, but strong $|n\rangle$ to $|n\rangle$ (carrier) stimulated Raman transitions, as well as by the sinusoidally-varying lattice-induced shift of the optical transition. This spatial variation of fluorescence is what provides us with a signal to detect an ion's position with sub-lattice-site resolution. The coupling from $|n\rangle$ to $|n-1\rangle$ and $|n-2\rangle$ also varies sinusoidally with the lattice, resulting in variations in cooling efficiency and a q-dependent temperature (see below).

Effects of Temperature on Friction

The temperature of the system can have a significant effect on stick-slip processes due to thermally induced hopping between two potential minima. In our system, the temperature is regulated by means of laser cooling, providing a dissipation mechanism to remove the heat released in the slip process. By the fluctuation-dissipation theorem, the ion follows a thermal distribution characterized by temperature T and a damping rate r. One can define a dimensionless ratio $\kappa = r \cdot \exp(-U/(k_B T))/(v/a)$ of the thermal hopping rate over the bare lattice potential barrier U to the driven transport rate over one lattice site at velocity v. When $\kappa \gg 1$, stick-slip is pre-empted by thermal hopping between the sites and its effect is much reduced. To observe stick-slip in deterministic transport, thermal hopping must be negligible ($\kappa \ll 1$), which we achieve by making the temperature low $k_B T \ll U$, and by choosing the transport speed v/a high enough. Since r^{-1} is the characteristic time constant for recooling after a slip, the transport speed must be slower than this to avoid raising the temperature, so we operate in the regime $\exp(-U/(k_B T)) \ll (v/a)/r \ll 1$.

We measure $U/(k_B T)$ independently by the equilibrium fluorescence of the middle ion in the crystal, placed at a minimum (node) of the optical lattice. As the ion thermally samples the optical potential near the minimum, it scatters light proportional to its temperature due to the laser cooling configuration (*23*). For $N = 3$ (data presented in Fig.3), the temperature for the $q = 0$ case is measured to be at most twice the temperature for the $q = 1$ case, where $k_B T(q=1)/U \approx 0.05$. If we increase the temperature for the $q = 1$ case (by introducing excess recoil heating via slight polarization misalignment of the optical pumping beam used for the Raman cooling process (*23*)) to match that of the $q = 0$ case, we find the measured friction to be reduced only by a factor of 2, by much less than the over tenfold reduction in the measured friction when changing the mismatch from $q = 1$ to $q = 0$. From this we conclude that temperature alone cannot explain the observed reduction in stick-slip friction. We note that although this temperature measurement is insensitive to the temperature of those vibrational modes of the crystal which do not contribute to the oscillation of the middle ion (such as the stretch mode for $N = 3$), those normal modes also do not contribute to the slip of the middle ion: in the matched case, all ions slip at once, corresponding to the center-of-mass mode, while in the mismatched case, ions slip one at a time, corresponding to a localized mode, and the temperature of the relevant mode for the middle ion is measured when this ion is placed at the optical lattice minimum.

In order to further assess the effects of temperature on friction when the structural mismatch q is tuned (Fig.4), we numerically simulate the full dynamics for crystals of different N. Using the Langevin formalism for the equations of motion subject to a fluctuating force (*1*), we obtain the q-dependence of friction for different temperatures. We find that in order to reproduce our experimental data, a q-dependent temperature is required. This is not unexpected from our cooling configuration (*23,31*), because the

cooling efficiency changes depending on an ion's location in the optical potential, and q tunes the arrangement of the ions relative to the optical potential. In the matched case, $k_B T(q=1)/U \approx 0.05$ is measured, while in the mismatched case, $k_B T(q=0)/U = 0.15$, as the only free parameter, produces good agreement with experimental data for $N=2$ through 6, indicating that the effect of mismatch on temperature is insensitive to the ion number. For intermediate matching values q we assume that the temperature increases linearly from $q=1$ to $q=0$.

We note that as the ion crystal is displaced by the applied force, because of the spatially-dependent cooling the temperature may change from the value measured with the middle ion at the optical lattice minimum. However, our simulations show that friction in the matched case $q=1$ is highly insensitive to temperature, and we use the $q=1$ measured temperature as input to the simulations. In the mismatched case $q=0$ our static temperature measurement may indeed underestimate the relevant temperature in the driven situation, which may be the cause of the discrepancy between the measured $k_B T(q=0)/U \approx 0.10$ and the fitted $k_B T(q=0)/U = 0.15$ temperature values.

Controlling the q parameter

The structural mismatch parameter q is measured by imaging the ion crystal as it is transported across the optical lattice in the regime where temperature dominates ($\kappa \gg 1$), and the optical-lattice potential is weak $\eta \approx 1$. In this way, the fluorescence signal from each ion reflects its average position relative to the optical-lattice potential, minimally perturbed by the optical force (aided by thermal averaging). We use these measurements to calibrate the Paul trap vibrational frequency ω_0 corresponding to the minimum value of q, and from there on use calculated values of q corresponding to the control parameter ω_0 and the given N. The calculated q versus ω_0 is periodic for $N=2$ and 3, but quasi-periodic for $N \geq 4$ (see Fig.S1) due to the inhomogeneity of the ion crystal. As a result, arbitrary tuning of q with the single parameter ω_0 becomes difficult with larger N (the value of q does not fully reach unity for $N=6$ and only gets to 0.75 for $N=10$ in the vicinity of the desired ω_0, as shown in Fig.5). For future experiments with larger ion numbers, this can to some extent be rectified by controlling quartic and higher-order Paul trap potentials available in our system (*27*), while for very large N near-square-well potentials with approximately constant ion spacings can be created by means of additional control electrodes.

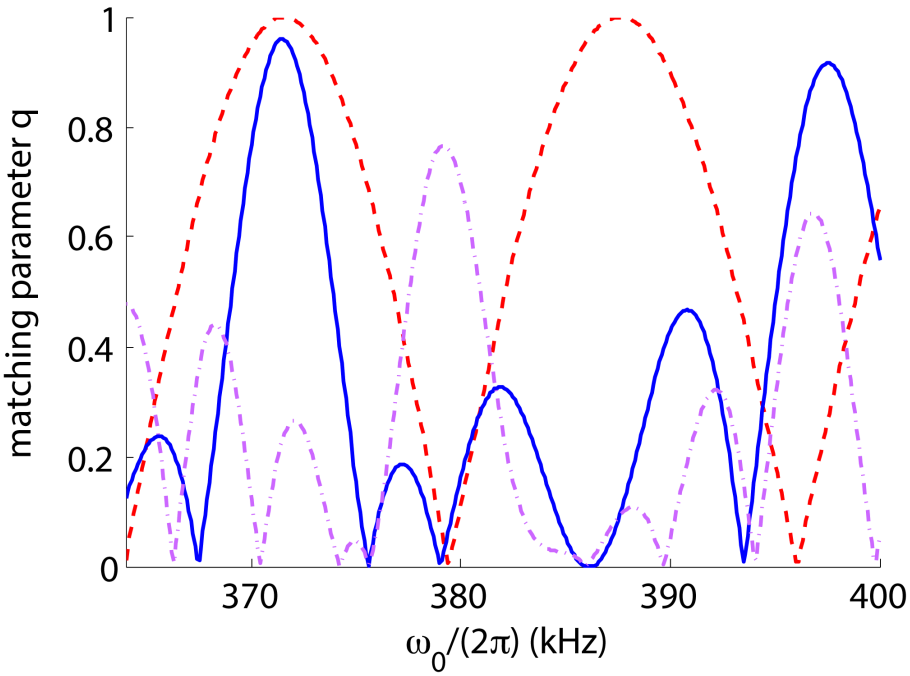

Fig. S1.

Calculated matching parameter q as a function of the Paul trap longitudinal vibrational frequency ω_0 for $N = 2$ (red dashed line), $N = 6$ (blue solid line) and $N = 10$ (purple dot-dashed line).

References

1. A. Vanossi, N. Manini, M. Urbakh, S. Zapperi, E. Tosatti, Colloquium: Modeling friction: From nanoscale to mesoscale. *Rev. Mod. Phys.* **85**, 529–552 (2013). doi:10.1103/RevModPhys.85.529

2. M. Urbakh, J. Klafter, D. Gourdon, J. Israelachvili, The nonlinear nature of friction. *Nature* **430**, 525–528 (2004). Medline doi:10.1038/nature02750

3. V. Bormuth, V. Varga, J. Howard, E. Schäffer, Protein friction limits diffusive and directed movements of kinesin motors on microtubules. *Science* **325**, 870–873 (2009). Medline doi:10.1126/science.1174923

4. C. H. Scholz, Earthquakes and friction laws. *Nature* **391**, 37–42 (1998). doi:10.1038/34097

5. K. Shinjo, M. Hirano, Dynamics of friction: Superlubric state. *Surf. Sci.* **283**, 473–478 (1993). doi:10.1016/0039-6028(93)91022-H

6. L. Prandtl, Ein Gedankenmodell zur kinetischen Theorie der festen Körper. *Z. Angew. Math. Mech.* **8**, 85–106 (1928). doi:10.1002/zamm.19280080202

7. G. A. Tomlinson, CVI. *A molecular theory of friction*. *Philos. Mag.* **7**, 905–939 (1929). doi:10.1080/14786440608564819

8. O. M. Braun, Y. S. Kivshar, *The Frenkel-Kontorova Model: Concepts, Methods, and Applications* (Springer, New York, 2004).

9. Y. I. Frenkel, T. A. Kontorova, *Zh. Eksp. Teor. Fiz.* **8**, 1340 (1938).

10. S. Aubry, The twist map, the extended Frenkel-Kontorova model and the devil's staircase. *Physica D* **7**, 240–258 (1983). doi:10.1016/0167-2789(83)90129-X

11. G. Binnig, C. F. Quate, C. Gerber, Atomic force microscope. *Phys. Rev. Lett.* **56**, 930–933 (1986). Medline doi:10.1103/PhysRevLett.56.930

12. C. M. Mate, G. M. McClelland, R. Erlandsson, S. Chiang, Atomic-scale friction of a tungsten tip on a graphite surface. *Phys. Rev. Lett.* **59**, 1942–1945 (1987). Medline doi:10.1103/PhysRevLett.59.1942

13. R. W. Carpick, M. Salmeron, Scratching the surface: Fundamental investigations of tribology with atomic force microscopy. *Chem. Rev.* **97**, 1163–1194 (1997). Medline doi:10.1021/cr960068q

14. I. Szlufarska, M. Chandross, R. W. Carpick, Recent advances in single-asperity nanotribology. *J. Phys. D* **41**, 123001 (2008). doi:10.1088/0022-3727/41/12/123001

15. A. Socoliuc, R. Bennewitz, E. Gnecco, E. Meyer, Transition from stick-slip to continuous sliding in atomic friction: Entering a new regime of ultralow friction. *Phys. Rev. Lett.* **92**, 134301 (2004). Medline doi:10.1103/PhysRevLett.92.134301

16. M. Dienwiebel, G. S. Verhoeven, N. Pradeep, J. W. Frenken, J. A. Heimberg, H. W. Zandbergen, Superlubricity of graphite. *Phys. Rev. Lett.* **92**, 126101 (2004). Medline doi:10.1103/PhysRevLett.92.126101

17. M. Hirano, K. Shinjo, R. Kaneko, Y. Murata, Observation of superlubricity by scanning tunneling microscopy. *Phys. Rev. Lett.* **78**, 1448–1451 (1997). doi:10.1103/PhysRevLett.78.1448

18. T. Bohlein, J. Mikhael, C. Bechinger, Observation of kinks and antikinks in colloidal monolayers driven across ordered surfaces. *Nat. Mater.* **11**, 126–130 (2011). Medline doi:10.1038/nmat3204

19. I. García-Mata, O. V. Zhirov, D. L. Shepelyansky, Frenkel-Kontorova model with cold trapped ions. *Eur. Phys. J. D* **41**, 325–330 (2007). doi:10.1140/epjd/e2006-00220-2

20. A. Benassi, A. Vanossi, E. Tosatti, Nanofriction in cold ion traps. *Nat. Commun.* **2**, 236 (2011). Medline doi:10.1038/ncomms1230

21. D. Mandelli, A. Vanossi, E. Tosatti, Stick-slip nanofriction in trapped cold ion chains. *Phys. Rev. B* **87**, 195418 (2013). doi:10.1103/PhysRevB.87.195418

22. T. Pruttivarasin, M. Ramm, I. Talukdar, A. Kreuter, H. Häffner, Trapped ions in optical lattices for probing oscillator chain models. *New J. Phys.* **13**, 075012 (2011). doi:10.1088/1367-2630/13/7/075012

23. L. Karpa, A. Bylinskii, D. Gangloff, M. Cetina, V. Vuletić, Suppression of ion transport due to long-lived subwavelength localization by an optical lattice. *Phys. Rev. Lett.* **111**, 163002 (2013). Medline doi:10.1103/PhysRevLett.111.163002

24. R. B. Linnet, I. D. Leroux, M. Marciante, A. Dantan, M. Drewsen, Pinning an ion with an intracavity optical lattice. *Phys. Rev. Lett.* **109**, 233005 (2012). Medline doi:10.1103/PhysRevLett.109.233005

25. M. Enderlein, T. Huber, C. Schneider, T. Schaetz, Single ions trapped in a one-dimensional optical lattice. *Phys. Rev. Lett.* **109**, 233004 (2012). Medline doi:10.1103/PhysRevLett.109.233004

26. D. Leibfried, R. Blatt, C. Monroe, D. Wineland, Quantum dynamics of single trapped ions. *Rev. Mod. Phys.* **75**, 281–324 (2003). doi:10.1103/RevModPhys.75.281

27. M. Cetina, A. Bylinskii, L. Karpa, D. Gangloff, K. M. Beck, Y. Ge, M. Scholz, A. T. Grier, I. Chuang, V. Vuletić, One-dimensional array of ion chains coupled to an optical cavity. *New J. Phys.* **15**, 053001 (2013). doi:10.1088/1367-2630/15/5/053001

28. Materials and methods are available as supplementary material on *Science* Online.

29. S. N. Medyanik, W. K. Liu, I.-H. Sung, R. W. Carpick, Predictions and observations of multiple slip modes in atomic-scale friction. *Phys. Rev. Lett.* **97**, 136106 (2006). Medline doi:10.1103/PhysRevLett.97.136106

30. J. Mizrahi, C. Senko, B. Neyenhuis, K. G. Johnson, W. C. Campbell, C. W. Conover, C. Monroe, Ultrafast spin-motion entanglement and interferometry with a single atom. *Phys. Rev. Lett.* **110**, 203001 (2013). Medline doi:10.1103/PhysRevLett.110.203001

31. V. Vuletić, C. Chin, A. Kerman, S. Chu, Degenerate raman sideband cooling of trapped cesium atoms at very high atomic densities. *Phys. Rev. Lett.* **81**, 5768–5771 (1998). doi:10.1103/PhysRevLett.81.5768